overall efficiency of such a system thus would not be limited to the fraction of the electrons' energy convertible to radiation in a single pass through the interaction region. The feasibility of the idea hinges on the form of the electrons' phase-space distribution after passage through the periodic field, a subject currently under study.

An electron current of the order of 1 A at 240 MeV would be sufficient for laser operation at 1000 Å for a 1-mm$^2$ electron-beam cross section. The measurements indicate that 0.2% of the electrons' energy can be converted to radiation in the periodic field without evidence of saturation; the corresponding power output for a 1-A, $10^8$-eV electron beam would exceed $10^5$ W.

We gratefully acknowledge the contributions of the Hansen Laboratory personnel and others who have assisted in this effort.

*Work supported in part by the U. S. Air Force Office of Scientific Research.

[1]J. M. J. Madey, J. Appl. Phys. 42, 1906 (1971).

[2]J. M. J. Madey, H. A. Schwettman, and W. M. Fairbank, IEEE Trans. Nucl. Sci. 20, 980 (1973).

[3]While the published Compton-scattering gain formulas can be reduced to a common functional form, the numerical factors are such that the predicted gains differ by up to two orders of magnitude.

[4]H. Dreicer, Phys. Fluids 7, 735 (1964).

[5]R. H. Pantell, G. Soncini, and H. E. Puthoff, IEEE J. Quantum Electron. 4, 905 (1968).

[6]V. P. Sukhatme and P. A. Wolff, J. Appl. Phys. 44, 2331 (1973).

[7]N. Kroll, in Stanford Research Institute Technical Report No. JSR-74-1, 1975 (unpublished), p. 74.

[8]J. L. Hirshfield, I. B. Bernstein, and J. M. Wachtel, IEEE J. Quantum Electron. 1, 237 (1965).

[9]V. L. Granatstein, M. Herndon, R. K. Parker, and S. P. Schlesinger, IEEE Trans. Microwave Theory Tech. 22, 1000 (1974).

[10]P. Sprangle, V. L. Granatstein, and L. Baker, Phys. Rev. A 12, 1697 (1975).

[11]R. L. Abrams, IEEE J. Quantum Electron. 8, 838 (1972).

[12]The Stanford-Princeton ring stored a peak current of 15 A at 300 MeV [W. C. Barber, High Energy Physics Laboratory Report No. 350 (unpublished)]. The SPEAR ring at SLAC has stored a peak current in excess of 100 A [H. Winick, SLAC Report No. 1349 (unpublished)].

# Detection of Brillouin Backscattering in Underdense Plasmas*

John J. Turechek and Francis F. Chen
*Electrical Sciences and Engineering Department, University of California, Los Angeles, California 90024*
(Received 16 September 1975)

Two new results are reported: (1) verification of the finite-interaction-length threshold for stimulated Brillouin scattering in a plasma with no critical layers, and (2) use of the time-dependent Stark effect to detect ion-frequency electric fields in a plasma.

Numerous theorists[1-4] have predicted that intense laser radiation $(\omega_0, \vec{k}_0)$ used to heat a plasma or implode a pellet may undergo parametric decay into an acoustic wave $(\omega_i, \vec{k}_i)$ and a backscattered light wave $(\omega_1, \vec{k}_1)$, resulting in reflection of the incident energy in the underdense, outer regions of the plasma, and thus diminishing absorption at the critical layer, where $\omega_0 = \omega_p \equiv (4\pi ne^2/m)^{1/2}$ or $n = n_c \equiv m\omega_0^2/4\pi e^2$. This process of stimulated Brillouin scattering (SBS) has a lower threshold[1] and higher nonlinear saturation[2] than the competing decay into a backscattered wave and an electron plasma wave (stimulated Raman scattering). The practical threshold depends on the finite interaction length[3] and the plasma inhomogeneity.[4] Recent high-power measurements[5] on solid targets indicate an increase in backscattered power with incident power $I_0$ up to $10^{15}$ W/cm$^2$, but a decrease thereafter; the latter has been attributed to a decrease in plasma scale length with intensity.[6] Because solid-target experiments are complicated by plasma formation and expansion and by reflection and absorptive parametric processes occurring at the critical $(\omega_0 = \omega_p)$ and quarter-critical $(\omega_0 = 2\omega_p)$ layers, we have designed an experiment to test the basic finite-length linear SBS theory under conditions in which the plasma is independently created and is everywhere underdense $(n < n_c/4$ or $\omega_0 > 2\omega_p)$. Our previously reported observations[7] have been confirmed by direct detection of the low-frequency field by means of the time-dependent Stark ef-

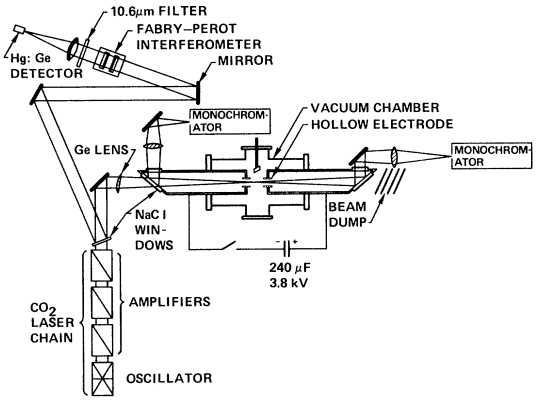


FIG. 1. Diagram of experiment.

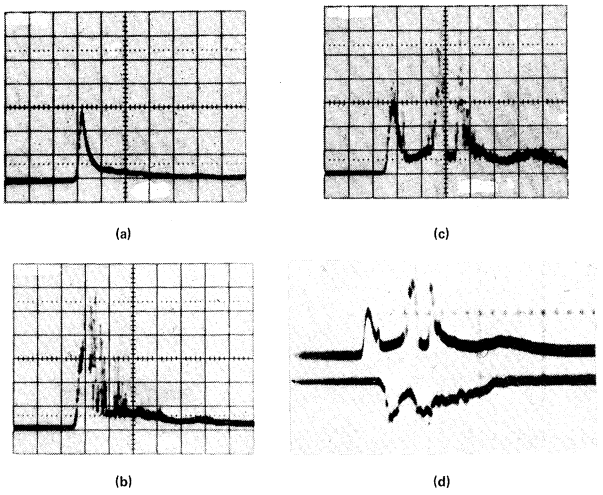


FIG. 2. Backscattering signals: (a) 10.6-μm stray light (plasma off); (b) typical backscattered plus stray light (plasma on); (c) same; (d) top trace: same pulse as (c) on two-beam scope; bottom trace: 6632-Å forbidden line signal (inverted). Sweep: 200 nsec/div.

fect.

Figure 1 shows the experimental arrangement. The plasma is created by a 30-kA discharge between tubular electrodes, 1.9 cm i.d. and 10 cm apart, both with and without a 4-kG stabilizing magnetic field. The 45-J, 0.5-GW double-discharge $CO_2$ oscillator-amplifier laser system produces a 3.2-cm-diam, 10.6-μm beam, which is focused by a 75-cm-focal-length Ge lens to a region 0.1 cm in diameter and 3 cm long in which the peak intensity has the approximately uniform value $5\times10^{10}$ W/cm$^2$. Backscattered radiation is collected by the same lens and sent via an NaCl beam splitter to an Hg:Ge detector after spectral analysis by a Fabry-Perot interferometer. Stray light is $10^{-9}$ of incident power and sets the detection threshold. Properties of the plasma before it is hit by the laser pulse are measured by spectroscopy (Stark broadening and line ratios), He-Ne interferometry, and double probes.

Numerous frequency scans have been made in He, Ar, and He seeded with Ar. Typical signals from the backscattering detector are shown in Fig. 2. The stray light signal in Fig. 2(a) indicates the incident pulse shape. Brillouin backscattering is seen as a series of short bursts with about 50 W peak power, occurring after the peak in $I_0$, the delay increasing with decreasing density. This delay is interpreted as due to laser heating of the electrons, without which the SBS threshold would be beyond the available power. The spiked character of the signal is caused by the subnanosecond growth time of the instability coupled with a rapid decay, probably due to shifts in $\omega_0$ and $I_0$ caused by axial mode jumping and self-mode-locking. In addition to SBS, the backscattered signal often shows a smooth peak occurring 200–1000 nsec after the peak in $I_0$, when the incident power is extremely small [see Fig. 2(c)]. This delayed signal neither correlates with forbidden-line emission (cf. next paragraph) nor shows a frequency shift[8] and is tentatively attributed to refraction or filamentation of the $CO_2$ light by the disturbed plasma, causing the transmitted light to miss the beam dump. Figure 3 shows examples of spectra of the time-integrated backscattered power after subtraction of the stray light and delayed signals. The frequency shifts correspond to $ZKT_e$ values of (a) 1400 eV, (b) 180 eV, and (c) 160 eV, where $-\Delta\omega=\omega_i=k_i c_s\simeq 2k_0(ZKT_e/M)^{1/2}$.

As a further check that SBS was indeed occurring, the low-frequency field at $\omega_i$ was detected directly by the time-dependent Stark effect,[9] in which a forbidden transition in He I is induced by the electric field. Using the NaCl Brewster windows as beam splitters, two optical channels were carefully adjusted to sample precisely the same focal volume as is illuminated by the $CO_2$ beam, as shown in Fig. 1. To achieve alignment, a Lucite plate is inserted into the focal region, and a small pit is burned in it with a single attenuated pulse from the $CO_2$ oscillator. The pit is illuminated with a He-Ne laser, and the steering mirrors are turned until the 0.5-m monochromators show maximum output at 6328 Å. In operation, one channel is tuned to the $3^1P$-$2^1P$ forbidden line at 6632 Å, while the other monitors either the continuum or the $3^1D$-$2^1P$ allowed line at 6678 Å. In Fig. 2(d), the 6632-Å forbidden-

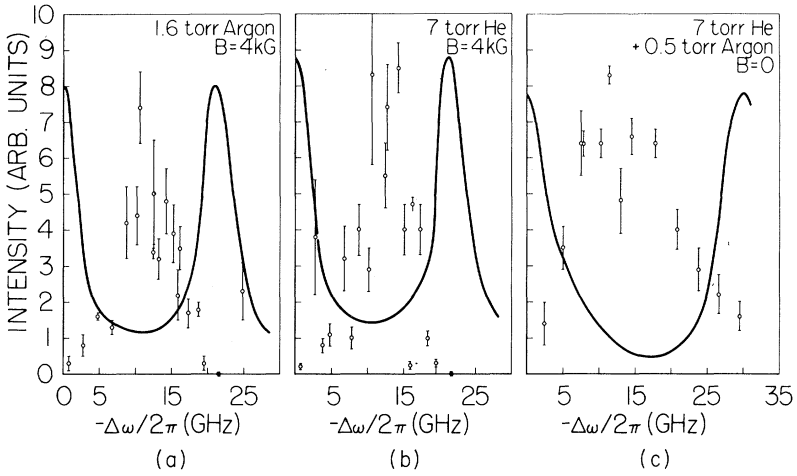


FIG. 3. Intensity of backscattered light versus red shift. Bars indicate probable error of the mean of several shots. Curves are scans of stray light and indicate finesse and free spectral range of the interferometer.

line signal shows two peaks: The first is correlated with the peak in incident (or stray) light, and the second with the occurrence of backscattering. The first peak cannot be used because ionization by the laser causes a general increase in background (as seen in the monitor channel), and the effect of prompt backscattering is masked. The second peak, delayed from the backscattering by the 80-nsec photomultiplier lag, is meaningful; it appears on the forbidden line only when backscattering occurs and only when the focal volumes are correctly aligned. The allowed line shows a smaller increase (due to a rise in continuum emission), with the net result that the ratio $S_{\pm}$, defined below, increases by about a factor of 2 during backscattering. The 6.4-Å slit width ensures that the detected transition is induced by a low-frequency field. The forbidden-line splitting due to a 10-GHz ion wave is $\Delta\lambda = \pm 0.15$ Å, while that due to Raman scattering would be ± 29 Å, and that due to the laser field at $\omega_0$ would be ± 443 Å.

To estimate the magnitude of fields involved, we evaluate the expression[9]

$$S_{\pm} = \hbar^2 \langle E_{1f}^2 \rangle R_{ll'}/6m^2e^2(\Delta \pm \omega_i)^2, \quad (1)$$

where $S_{\pm}$ is the ratio of satellite-line to allowed-line intensity, $\langle E_{1f}^2 \rangle$ is the mean square low-frequency electric field, $R_{ll'}$ is a constant equal to 40 for the 6632-Å line, and $\Delta$ is the angular-frequency equivalent of the 6678-6632-Å difference. Previous calculations[10] of the ordinary Stark effect indicate that $S_{\pm} \simeq 0.02$ for the 6632-Å line under our experimental conditions, and we assume that this background level is doubled by $E_{1f}$. Taking both satellites into account, we then obtain $\langle E_{1f}^2 \rangle = (96\ \mathrm{kV/cm})^2$ as a detection threshold. If $I_0 = 5 \times 10^9$ W/cm$^2$ and $I_1 = 10^{-6} I_0$ from the measured incident and backscattered powers during the tail of the pulse, then $E_0 = 435$ kV/cm and $E_1 = 1.4$ kV/cm rms. The high-frequency average $\langle (E_0 + E_1)^2 \rangle$ has a beat-frequency component of amplitude $2\langle E_0 E_1 \rangle = (44\ \mathrm{kV/cm})^2$ at the ion frequency. This is of the right order of magnitude.[11] The time correlation of 6632-Å emission with SBS is what makes detection unmistakable even at this marginal amplitude.

Maximum backscattering occurs not at peak discharge current but at about 18 $\mu$sec after firing. Auxiliary diagnostics suggest the following sequence in He: The initial discharge is hollow, $n_e$ having a maximum at the i.d. of the tubular electrodes. At $t_0$, when the laser pulse is fired, the density on axis has filled in to a value $5 \times 10^{16}$ cm$^{-3}$, while the neutral density is still $\sim 1.5 \times 10^{17}$ cm$^{-3}$. At this time, $KT_e = 6$ eV and $KT_i \simeq 3$ eV. The initial spike of the laser pulse heats the electrons classically and completes the ionization to $Z = 2$, bringing $n_e$ to $\sim 4 \times 10^{17}$ cm$^{-3}$. The temperature at peak power is limited by radial heat conduction; it was not measured but was calculated to be 63 eV. This is in reasonable agreement with the observed red shifts, which gave $KT_e \sim 80$ eV for He ($Z = 2$). For argon, one expects $Z = 8$ and $KT_e = 110$ eV, while the shift in Fig. 3(a) indicates 175 eV.

Finally, we consider the threshold. The relevant formula is given by Pesme, Laval, and Pellat[3] for the convective instability of damped ion waves in a finite medium[12]: $N = \gamma_0^2 l/c\gamma_i$, where $N$ is the minimum detectable number of $e$ foldings

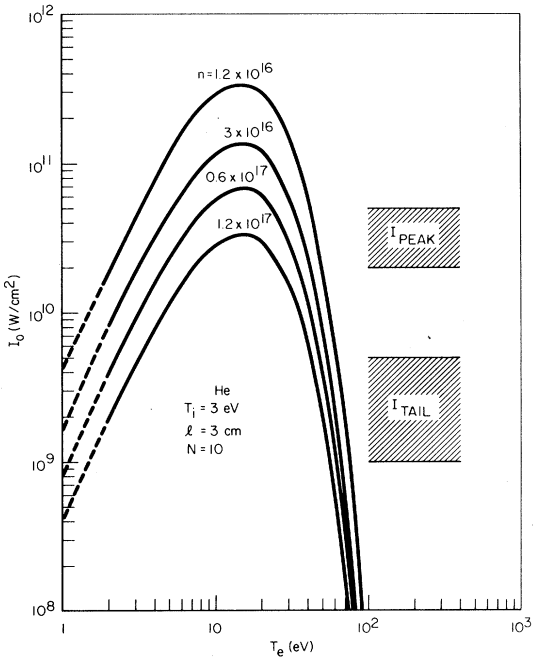


FIG. 4. Theoretical threshold intensity $I_0$ versus $KT_e$ for various $n_e$ (in $\mathrm{cm}^{-3}$). The ranges of experimental values of $I_0$ in the peak and the tail of the pulse are shown.

above the initial ($\simeq$thermal) ion-wave level, $\gamma_0$ is the intrinsic growth rate, $l$ is the interaction length, $c$ is the velocity of light, and $\gamma_i$ is the ion-wave damping rate. Inserting the well-known result[1,12] for $\gamma_0$ and using for $\gamma_i$ the asymptotic expression for ion Landau damping (valid for $T_e/T_i > 2$), we obtain for He at threshold

$$I_0(\mathrm{W/cm^2}) = 4\times 10^{26} N f(T_e)/n_e l, \qquad (2)$$

where

$$f(T_e) = KT_e(T_e/T_i)^{3/2}\exp[-\tfrac{1}{2}(3+T_e/T_i)].$$

$I_0(T_e)$ is plotted in Fig. 4 for $KT_i = 3$ eV, $N = 10$, $l = 3$ cm; $f(T_e)$ has a maximum value $\simeq KT_i$ eV at $T_e = 5T_i$. It is seen that $I_0$ at the initial condition of $n_e = 5\times 10^{16}$ $\mathrm{cm}^{-3}$ and $KT_e = 6$ eV is just above the available intensity. Only after $n_e$ and $T_e/T_i$ are increased by laser heating ($T_i$ does not change during the pulse) does the threshold fall within reach. When $KT_e$ rises above about 50 eV, Landau damping is so small that even intensities in the tail of the pulse are above threshold, as is observed. The correctness of the magnitude of the theoretical threshold (2) is borne out by the large shot-to-shot variation in backscattering, resulting from minor fluctuations in the exponentiation factor $N$, which shows that the experiment is at marginal stability.

The thermal level of ion waves would give a scattered power of 5 mW into the detector. A typical observed power of 50 W therefore corresponds to 9 $e$ foldings (hence, $N \simeq 10$ was assumed above). Using the formula[13]

$$\frac{dW}{dt\,d\Omega\,d(\omega/2\pi)} = I_0 V\sigma_T(\theta,\varphi)\lim_{T,V\to\infty}\left(\frac{2}{TV}|n_1(\vec{k},\omega)|^2\right), \qquad (3)$$

one calculates that the ion wave responsible for the observed SBS has amplitude $n_1/n_0 \simeq 1.7\times 10^{-6}$, or $E \simeq 1.2$ V/cm. This is too small to be directly observable by the Stark effect.

In conclusion, we have verified the predictions of SBS theory in plasmas by (a) checking the frequency shift, (b) checking the magnitude of the threshold, and (c) detecting the beat-frequency field spectroscopically. A complete study of the forbidden-line diagnostic, including a scan of the line profile, was not possible because of poor reproducibility; further work with laser intensities well above threshold is strongly suggested. Even in its rudimentary state, this diagnostic enabled us to reject certain spurious signals as being irrelevant to SBS.

The assistance of Mark Herbst with the measurements is gratefully acknowledged.

*Work supported by U. S. Energy Research and Development Administration, Contract No. E(04-3)34, P. A. 157 and 236.

[1]J. F. Drake, P. K. Kaw, Y. C. Lee, G. Schmidt, C. S. Liu, and M. N. Rosenbluth, Phys. Fluids 17, 778 (1974).

[2]D. W. Forslund, J. M. Kindel, and E. L. Lindman, Phys. Rev. Lett. 30, 739 (1973); W. L. Kruer, K. G. Estabrook, and K. H. Sinz, Nucl. Fusion 13, 952 (1973).

[3]D. Pesme, G. Laval, and R. Pellat, Phys. Rev. Lett. 31, 203 (1973).

[4]M. N. Rosenbluth, Phys. Rev. Lett. 29, 565 (1972).

[5]L. M. Goldman, J. Soures, and M. J. Lubin, Phys. Rev. Lett. 31, 1184 (1973), and in *Proceedings of the Fifth International Conference on Plasma Physics and Controlled Nuclear Fusion Research, Tokyo, Japan, 1974* (International Atomic Energy Agency, Vienna, Austria, 1975), Paper No. CN-33-F4-2.

[6]W. L. Kruer, E. Valeo, and K. G. Estabrook, Phys. Rev. Lett. 35, 1076 (1975).

[7]J. J. Turechek and F. F. Chen, Bull. Am. Phys. Soc. 19, 919 (1974).

[8]A definitive spectrum could not be obtained because of poor reproducibility.

[9]M. Baranger and B. Mozer, Phys. Rev. 123, 25

(1961).
[10]B. Ya'akobi, E. V. George, G. Bekefi, and R. J. Hawryluk, J. Phys. B 5, 1017 (1972).
[11]Why this quantity should be used for $\langle E_{1f}{}^2\rangle$ of Eq. (1) is a nontrivial question. We do not preclude the possibility of a Stark effect stronger than that treated by Baranger and Mozer. In any case, neither the ion-wave field itself nor the equivalent electric field of the beat-frequency ponderomotive force is large enough to cause the observed effect.
[12]The inhomogeneous-plasma threshold is higher in this case. Thresholds and their meanings have been summarized by F. F. Chen, in *Laser Interaction and Related Plasma Phenomena*, edited by H. J. Schwarz and H. Hora (Plenum, New York, 1974), Vol. 3A, p. 291.
[13]G. Bekefi, *Radiation Processes in Plasmas* (Wiley, New York, 1966), p. 258.

# Brownian Motion near Hydrodynamic-Regime Transitions

H. N. W. Lekkerkerker
*Fakulteit van de Wetenschappen, Vrije Universiteit Brussel, 1050 Brussels, Belgium*

and

Jean-Pierre Boon*
*Faculté des Sciences, Université Libre de Bruxelles, 1050 Bruxelles, Belgium*

(Received 17 November 1975)

The diffusion coefficient of suspended Brownian particles diverges near a hydrodynamic-regime transition point.

Pretransitional phenomena in nonequilibrium systems evolving towards an instability point bear a striking resemblance to those occurring near equilibrium phase transitions.[1] One of the most interesting analogies is the amplification of the thermal fluctuations near the transition point. In particular the enhancement of the fluid velocity fluctuations induces an increase of the diffusion coefficient of Brownian particles suspended in the fluid. This was shown for the particular case of the convective instability[2] and is seen here to be a general feature of hydrodynamic-regime transitions.

The system considered is infinite in the $z$ direction and finite in the $x$ and $y$ directions; then the fluctuating fluid velocity field $\vec{v}(\vec{r}, t)$ can be written as

$$v_j(\vec{r}, t) = \sum_n \int dk v_j(n, k, t) e^{ikz} f_n(x, y), \quad j = x, y, z, \qquad (1)$$

where the expansion functions $f_n(x, y)$ are assumed to form a complete set and satisfy the boundary conditions. Near a hydrodynamic instability point, there is a branch of modes—say those with $n = 1$—which become unstable; their corresponding damping factor, $\lambda(1, k)$, can in general be written as[3]

$$\lambda(1, k) = \alpha\epsilon + \beta(k - k_c)^2. \qquad (2)$$

Here $\alpha$ and $\beta$ are merely expansion coefficients and $\epsilon = (R_c - R)/R_c$. $R$ is the parameter characterizing the nonequilibrium constraints on the system and $R_c$ denotes its critical value,[4] i.e., when $\epsilon \to 0$, the modes with wave number $k_c$ become unstable. Furthermore, in view of the analogy between regime transitions and phase transitions, $\lambda(1, k)$ can be cast into the form of an Ornstein-Zernike–type expression by rewriting Eq. (2) as

$$\lambda(1, k) = \alpha\epsilon[1 + \xi^2(k - k_c)^2], \qquad (3)$$

where $\xi$ denotes the correlation length, with $\xi \propto d\epsilon^{-1/2}$, $d$ being the characteristic dimension of the system. On the other hand, from the stochastic linear hydrodynamic equations describing the system, the correlation function of the fluid velocity fluctuations of the unstable branch is given by[5]

$$\langle v_j^*(1, k, 0) v_j(1, k', t)\rangle = \frac{C_j(k)}{\lambda(1, k)} e^{-\lambda(1,k)t}\,\delta(k - k'), \qquad (4)$$

where the explicit form of the quantity $C_j(k)$ depends on the specific problem considered.[6] It is clear from Eqs. (3) and (4) that when $\epsilon \to 0$ the fluctuations of the modes with $n = 1$ and with wave number $k \simeq k_c$ are amplified and decay very slow-

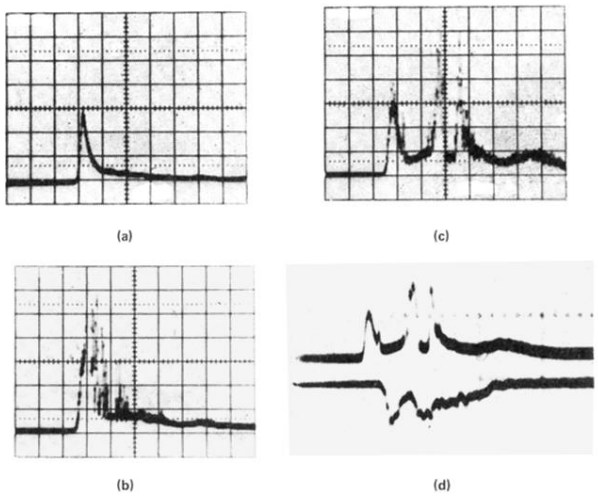


FIG. 2. Backscattering signals: (a) 10.6-$\mu$m stray light (plasma off); (b) typical backscattered plus stray light (plasma on); (c) same; (d) top trace: same pulse as (c) on two-beam scope; bottom trace: 6632-Å forbidden line signal (inverted). Sweep: 200 nsec/div.